Int. J. Electrochem. Sci., 14 **(2019)** 5637 – 5645, doi: 10.20964/2019.06.38

International Journal of ELECTROCHEMICAL SCIENCE
www.electrochemsci.org

Electrochemical Synthesis of Cu_xO/Cu_2S Nanocomposites as Nonenzymatic Glucose Sensor

Xue Xu[1], Huile Jin[1], Qian Ren[1], Aili Liu[1], Jun Li[1], Dewu Yin[1], Xin Feng[1], Xiaomei Dong[1], Jichang Wang[2,], Shun Wang[1,*]*

[1] College of Chemistry and Materials Engineering, Institute of New Materials and Industrial Technologies, Wenzhou University, Wenzhou, Zhejiang 325035, China
[2] Department of Chemistry and Biochemistry, University of Windsor, Windsor, ON N9B 3P4, Canada
[*]E-mail: shunwang@wzu.edu.cn, jwang@uwindsor.ca

Received: 2 January 2019/ *Accepted:* 21 February 2019 / *Published:* 10 May 2019

The focus of this study is to explore ways of accelerating the corrosion rate of copper anodes for the possible synthesis of copper nano-composites on the counter electrode, and the subsequent applications of such composites as nonenzymatic glucose sensor. Normally, a strong corrosion resistance of copper anodes emerges in alkaline solutions due to the formation of a passive copper hydroxide film, which prevents further corrosion. In this research the presence of sulfide ions in the electrolyte was found to dramatically promote the corrosion process and eventually led to the production of Cu_xO/Cu_2S (where Cu_xO was consist of Cu_2O and CuO) nanocomposites on the counter electrode during the electrochemical corrosion process. When the as-prepared copper nanocomposites electrodes were used to detect the oxidation of glucose, a strongly enhanced anodic process was obtained, in which the detection limit was found to be around 10 uM with a linear range of 10-1000 uM and a detection sensitivity of 2688 uA cm^{-2} mM^{-1}.

Keywords: electrochemical corrosion, copper nanocomposites, counter electrode, current oscillation, nonenzymatic glucose sensor

1. INTRODUCTION

The blood sugar level is a key factor for evaluating the health status of an individual, usually being tested for diabetes [1,2]. Conventional enzymatic glucose sensors have received much attention since 1962 for their quick detection and high sensitivity. However, enzymatic glucose sensors are restricted in clinical applications due to enzyme activity is unstable and environmentally sensitive to pH

and temperature [3,4]. In the past decade, nonenzymatic glucose sensors have been widely recognized as an ideal alternative due to their stability, safety, cost-effectiveness, high selectivity and sensitivity [5-7]. Most of the nonenzymatic glucose sensors are based on the current signal produced by the direct oxidation of glucose on the anodic electrodes [8,9]. Regarding the electrode materials, varied transition metal oxides [10-15] have been developed as efficient electrocatalysts for glucose sensing.

Among these metal oxides, copper oxide (CuO) is a research hotspot due to its tunable facet structure, suitable surface charge and excellent catalytic performance [16-18]. To date, CuO-based nanomaterials used in glucose sensors have been intensively studied, especially in the design multi-dimensional nanostructures [19-22]. For instance, our former study revealed that cubic facet favors the electro-oxidation of glucose rather than pyramid [19], and the combination of Cu_2O/CuO nanoparticles and carbon tubes produces synergistic electrocatalytic activity on glucose oxidation [20]. However, these structures were mostly achieved either via chemical reduction or from cathodic deposition. Few cases were numbered via in-situ anodic dissolution of copper and cathodic deposition of CuO, which may give rise to new design of CuO nanostructures. The failure is mainly due to the two electrochemical processes are hardly happened simultaneously. Because the anodic dissolution of copper in alkaline solutions is largely inhibited due to the formation of a passive copper oxide film, which prevents further corrosion and deposition of CuO on cathodes. On the other hand, acidic electrolytes are facilitating the corrosion processes, but the final deposits would be copper rather than CuO. Therefore, understanding the mechanism of electrochemical corrosion [23,24] is important for the new design of CuO nanocomposites. In the last two decades, the anodic passivation studies of copper in alkaline solutions have revealed a Cu_2O barrier layer adjacent to copper metal and an outer layer of precipitated $Cu(OH)_2$ is often formed [25,26]. However, the whole scenario of corrosion is complicated and needs to be further investigated under different chemical environments.

In this work, we demonstrate the copper corrosion process is greatly enhanced in the presence of sulfide ions. Sulfide ions are competing with hydroxide ions in the electrochemical absorption and corrosion process, however, sulfide ions can be easily oxidized into sulfates, making the barrier layer adjacent to copper metal disappeared and exposed again with the active copper sites for further corrosion. Thereafter, sufficient corroded Cu^{2+} ions are generated to support the deposition of copper oxides on the surface of counter electrode.

2. EXPERIMENTAL

2.1 Materials and apparatus

Copper foil, sodium acetate, sodium hydroxide, sodium sulfide were all purchased from Aladdin, China. All the chemical reagents were used without further purification. Deionized water was prepared with a Milli-Q purity system (18.2 M). X-ray diffraction (XRD) measurements were conducted on a Bruker D8 Advance diffractometer using Cu-Kα radiation (λ = 0.15406 nm), where the data was collected in the 2θ range of 10-90° with a step size of 0.02°. Scanning electron microscopy (SEM) was measured on a Nova Nanosem 200 system operated at an acceleration voltage of 15 kV. X-ray

photospectroscopy (XPS) was performed on a spectrometer from Kratos Axis Ultradld, using Mono Al Kα (1486.71 eV) radiation at a power of 120 W (8 mA, 15 kV).

2.2. Electrochemical synthesis of copper nanocomposites

Three-electrode system was applied in this study, where a copper foil, a platinum foil, and a saturated calomel electrode were employed as the working, counter, and reference electrodes, respectively. Potentiostatic measurements were performed at different applied corrosion potentials (0.45-0.65 V). In a typical synthesis, copper foil (8 mm × 3 mm) was applied as the copper precursor, and 7.6 mL of 0.01 M sodium sulfide (Na_2S) was pumped in 0.5 M sodium acetate (NaAC) as electrolyte dissolved in 50 mL water via a peristaltic pump, starting right after 100 s of the electrochemical dissolution and lasting for 3 hours. The as-obtained CuO deposits on counter electrode were isolated by ultrasonication and centrifugation in water and cleaned by water and ethanol for three times. The collection was finally dried in vacuum at 80℃ for 6 h for further usage and characterization.

2.3. Glucose sensing

To fabricate working electrodes for glucose sensing, 2 mg CuO materials were mixed with 100 uL ethanol, 400 uL water and 5 uL Nafion. Typically, 10 uL of the mixture was spread on a glassy carbon electrode with 3 mm diameter. Pt wire and saturated calomel electrode (SCE) were employed as the counter and reference electrodes, respectively. Cyclic voltammograms with a scan rate of 50 mV/s and amperometric i-t measurements were applied for glucose sensing. The calibration curve of glucose concentration versus current response is based on amperometric i-t response.

3. RESULTS AND DISCUSSION

Fig. 1 shows i-t curves of copper electrodes in a 0.5 M NaAc electrolyte solution at different applied potentials. Note that, as stated in the above experimental section, 0.01 M Na_2S solution was slowly pump into the reactor. Here, the passivation and corrosion kinetics resulted in the occurrence of simple oscillations in the anodic current. In the absence of Na_2S, no current oscillations were seen, highlighting the unique role of sulfide in removing the passivation layer. Here, a fast corrosion process (i.e., almost instant increase of corrosion current) was occurred, especially in Fig. 1b. Such a fast oxidation process is coupled with a slow passivation reaction, indicated by the graduate decrease of the anodic current. The oscillatory frequency is related to the degree of the corrosiveness of copper foil, in which at the applied potential of 0.55 V the corrosion is most obvious. In general, a slow corrosion frequency is assumed to be caused by the deposition of sulfur element on the copper surface, which arises from the oxidation of sulfide [27]. The temporary protection by sulfur coating is gradually faded by the afterward electro-oxidation of sulfur and further dissolution of copper.

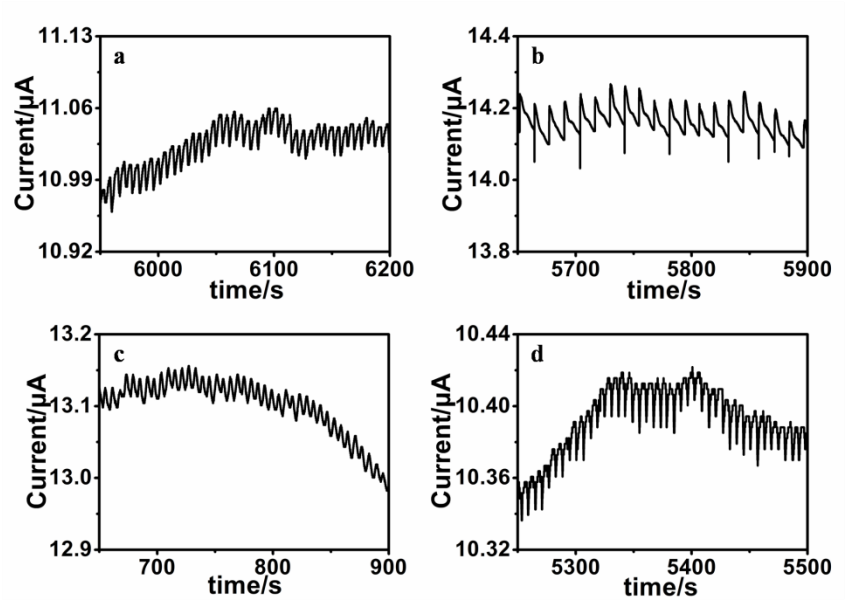

Figure 1. i-t curves under the different applied potential in 0.5mol L^{-1} NaAC solution, (a) 0.45 V, (b) 0.55 V, (c) 0.6 V, (d) 0.65 V.

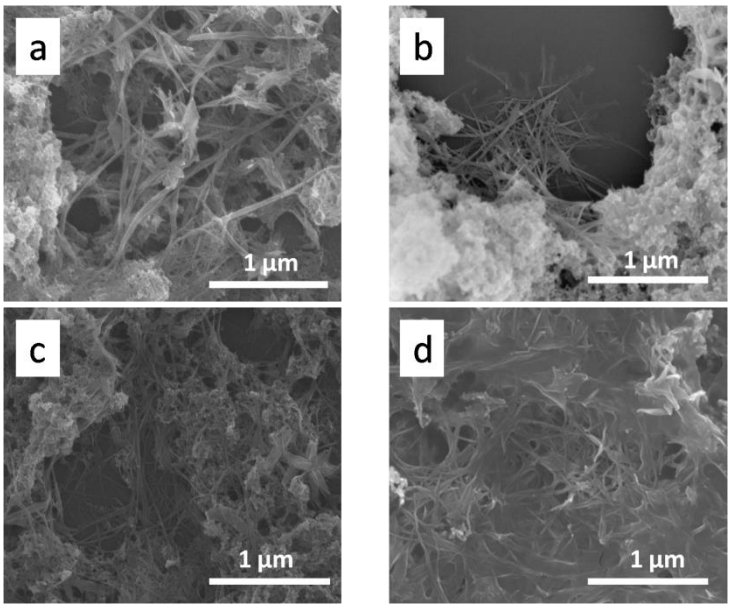

Figure 2. SEM images of the deposit formed at the counter electrode surface under the different potential, (a) 0.45 V, (b) 0.55 V, (c) 0.6 V, (d) 0.65 V.

The negative balancing potential at the counter electrode is expected to reduce H^+ to form bubbles or reduce Cu^{2+} ions to cause electrochemical deposition. Surprisingly, as shown in Fig. 2, solids with very different morphologies were deposited on the surface of platinum counter electrode in the presence of Na_2S. The following characterization with XRD and XPS indicates that the above deposit consists of copper oxides, suggesting that the reactions occurring on the counter electrode may involve an electrochemical adsorption of Cu^{2+} ions and the reduction of Cu^{2+} ions to Cu^+. After dried in the vacuum, copper oxides were obtained. Notably, control experiments without Na_2S, in which even though the pH

of the solution was compensated to be the same by adding 0.01 M NaOH into the NaAC solution, only yielded the steady current and clean surface of counter electrode. It is worth to note that different corrosion potentials result in very different morphologies, where rich with nano-clusters (Fig. 2a-c) rather than nano-sheets (Fig. 2d) could be seen.

XRD measurements in Fig. 3 further confirm that the copper species in the deposit formed at different applied potentials are different. Specifically, at the corrosion potentials of 0.45 V and 0.55 V, there is mainly CuO in the composites. As the corrosion potential was increased above 0.6 V, Cu_2O starts to appear in XRD curves, where Cu_2O is presumably from the reduction of Cu^{2+} ions to Cu^{+}. Trace amount of Cu_2S is also formed on the surface of platinum counter electrode, 1.4-2.1 at % of sulfur was confirmed by energy dispersive X-Ray analysis.

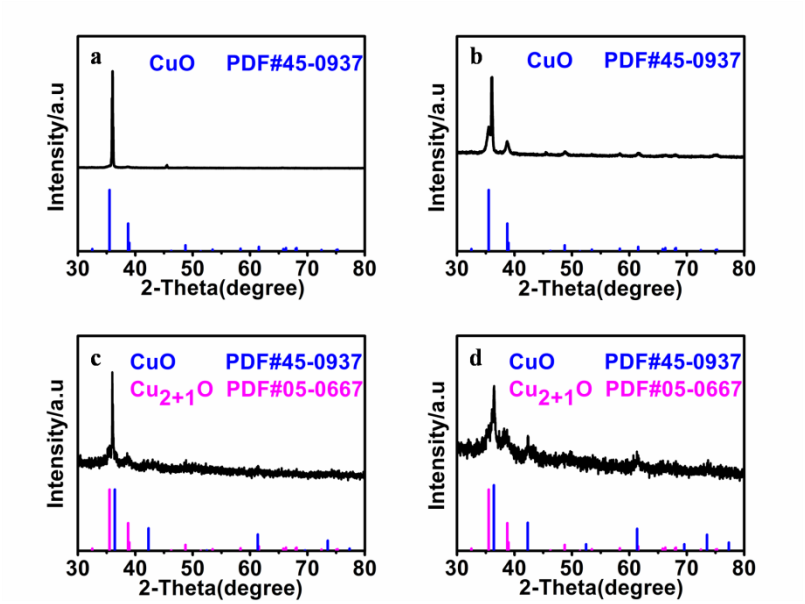

Figure 3. XRD patterns of the counter electrode surface, with the different potential, (a) 0.45 V, (b) 0.55 V, (c) 0.6 V, (d) 0.65 V.

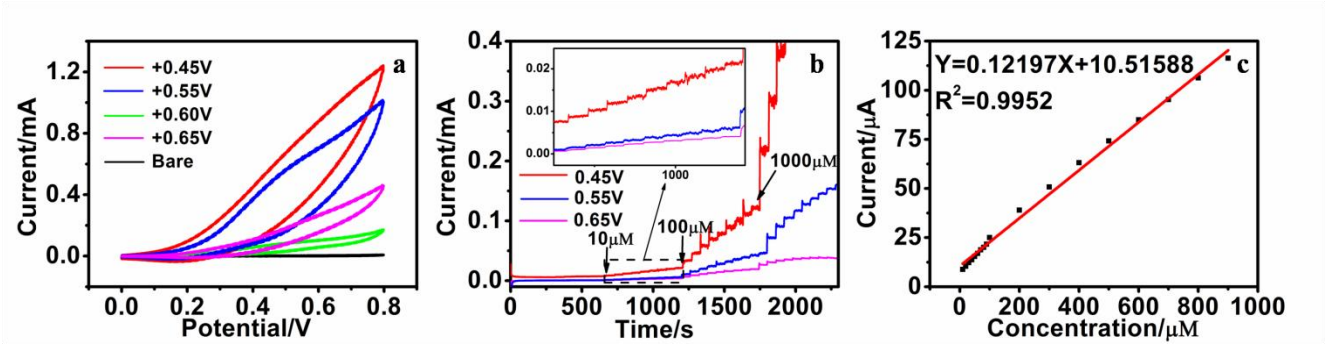

Figure 4. (a) Cyclic voltammograms electrodes that were prepared at different corrosion potentials, the electrolyte contains 10 mM glucose and 0.01 M NaOH, and scan rate of 50 mV/s, (b) amperometric response of the copper oxides in 0.01 M NaOH solutions with injection of different concentrations of glucose, and (c) The calibration curve of glucose concentration versus current response showing linear range at an applied potential of 0.45 V.

Table 1. Comparison of copper-based electrodes for glucose sensing in recent years.

Electrode	Sensitivity/ $\mu A\ cm^{-2}mM^{-1}$	Linear range/ mM	Detectionlimit/ μM	Reference
rGO/CuS nanoflakes	53.5	0.001-2	0.19	[28]
CuS microflower	1007	0.002-5.4	2.0	[29]
CuS	1085	0.02-2.5	2	[30]
$Cu_2O@Cu_{1.8}S$	3630	0.001-1	0.0678	[31]
Cu_2O mesoporous nanospheres	2116.9	0.003-7.8	0.42	[32]
CuO nanoplatelets	3490.7	upto 0.8	0.5	[33]
porous CuO	934.2	0.0005-2.8	0.1	[34]
CuO nanourchins	2682	-	1.52	[35]
CuO nanofibers	431.3	0.006-2.5	0.8	[36]
CuxO/Cu	1620	0-6	49	[37]
CuO nanowire arrays/copper wire	850.7 446.7	0.005-8.555	2.86	[38]
CuO	1322	0.001-4	0.5	[39]
CuO microflowers	3100	0.01-0.12	6.48	[40]
Cu_xO/Cu_2S Nanocomposites	2688	0.01-1	10	This work

Table 2. Recovery measurements for glucose sensing.

Samples setting up	Found[a] uM	RSD % n=3	Recovery %
500 uM glucose, 0.1 M NaOH	532.9	6.97	106
human serum 0.75 mM[b]	705.1	7.09	94

[a] average value of three rounded tests.
[b] blood glucose meter.

The preliminary study on the electrochemical detection of glucose was depicted in cyclic voltammograms (CV) as shown in Fig. 4a. The CV measurements were performed using different sensor that have been synthesized at different corrosion potentials. Comparing with the nearly flat CV of the bare electrode, the result clearly indicate that copper nanocomposites prepared in this study can significantly enhance the electro-oxidation of glucose. Meanwhile, the CVs also shows that the composites prepared at the low corrosion potential seems to have better electrocatalytic activity. To further confirm the activity of as-prepared glucose sensors, real time amperometric method was applied with injection of different concentrations of glucose in 0.01 M NaOH solution. It can be seen in Fig. 4b that the stepwise addition of glucose causes the increasing of current response, and the most efficient

and sensitive copper composites electrode that is synthesized at 0.45 V exhibits a linear range of 10-1000 uM with a correlation coefficient of R^2=0.995 in Fig. 4c. The detection limit was determined to be 10 uM.

In this work, the detection limit was found to be around 10 uM with a linear range of 10-1000 uM and a detection sensitivity of 2688 uA cm^{-2} mM^{-1}. To evaluate the sensitivity, linear range and detection limit of our fabricated copper nanocomposites with respect to other copper-based glucose sensors, Table 1 lists the most recently published copper-based glucose sensors [28-40]. The results indicate that our as-prepared Cu_xO/Cu_2S-based nonenzymatic glucose sensors exhibit attractive features, especially with an improved sensitivity. Such an observation indicates that the active components, specifically CuO, Cu_2O and Cu_2S, are highly active towards the electrochemical oxidation of glucose. Regarding the electrochemical oxidation mechanism of glucose on Cu_xO/Cu_2S electrode in alkaline medium, it is identical with that of $Cu_2O@Cu_{1.8}S$ materials [31]. In which, copper species can be oxidized to Cu^{3+} and further oxidizing glucose into gluconic acid. It is further found that $Cu_2O@Cu_{1.8}S$ materials possess a larger current response than that obtained on pure Cu_2O, indicating a better sensitivity towards glucose sensing on the active component of copper sulfides. In our experiment, we also found the similar evidence that Cu_xO/Cu_2S electrode prepared at 4.5 V possessed 2.1 at% of Cu_2S, which is more than that of Cu_xO/Cu_2S electrode prepared at 6.5 V (1.4 at%). As a result, a larger current response and thus a better sensitivity are occurred on the Cu_xO/Cu_2S electrode prepared at 4.5 V as shown in Fig. 4b, indicating Cu_2S can effectively access large number of glucose molecule and also improve the charge transfer between glucose and active electrode surface. Overall, trace amount of Cu_2S can significantly influence the electrochemical activity towards glucose oxidation.

To examine the feasibility of using this new platform inpractical applications, glucose determination in real human serum sample were also investigated in this research. As shown in Table 2, the sensor exhibits a good recovery rate. However, a moderate linear range and relatively high values of detection limit suggest that there is still a great room to optimize the performance. This may be done by tuning the active components of copper oxide/copper sulfide composites via nonlinear electrochemistry.

4. CONCLUSION

In summary, we have shown how the presence of sulfide in the electrolyte could accelerate the electrochemical corrosion of copper. The presence of sulfide is also responsible for the development of current oscillations in this studied system as well as the formation of deposit at the counter electrode. Interestingly, the morphology of the as-prepared copper nanocomposites appears to be dependent on the oscillatory behavior, providing an example on the application of nonlinear dynamics to the fabrication of nanomaterials. Our study on the corrosion behavior of Cu in aqueous NaAC-Na_2S solution also illustrates a non-negligible role of counter electrode. As a case study on the electrocatalytic activity of the synthesized copper nanocomposites, the as-obtained Cu_xO/Cu_2S materials was used to electrochemically oxidize glucose, which exhibits a good response for the nonenzymatic glucose sensing.

ACKNOWLEDGEMENTS

This work was supported by the National Natural Science Foundation of China (21628102 and 21601138), the Zhejiang Provincial Natural Science Foundation of China (LZ17E020002, LZ15E020002 and LY17E020003), Wenzhou Public Welfare Technology Project (project No. G20170018 and No. S20170004), Zhejiang Provincial College Students Science and Technology Innovation Program and Xinmiao Talents Program (2018R429063).

References

1. Y. C. Zhang, L. Su, D. Manuzzi, H. V. E. Monteros, W. Z. Jia, D. Q. Huo, C. J. Hou, Y. Lei, *Biosens. Bioelectron.,* 31 (2012**)** 426-432.
2. C. Batchelor, G. G. Wildgoose, R. G. Compton, L. D. Shao, M. L. H. Green, *Sens. Actuators, B.,* 132 (2008) 356-360.
3. L. Na, C. L. Shao, X. H. Li, F. J. Miao, K. X. Wang, Y. C. Liu, *Ceram. Int.,* 42 (2016**)** 11285-11293.
4. W. N. Xu, S. G. Dai, X. Wang, X. M. He, M. J. Wang, Y. Xi, C. G. Hu, *J. Mater. Chem. B.,* 3 (2015) 5777-5785.
5. J. Yang, W. D. Zhang, S. Gunasekaran, *Biosens. Bioelectron.,* 26 (2011) 279-284.
6. D. Martín-Yerga, J. Carrasco-Rodríguez, J. L. G. Fierro, F. J. G. Alonso, A. Costa-García, *Electrochim. Acta,* 229 (2017) 102-111.
7. N. Wang, Z. W. Han, H. Fan, S. Y. Ai, *RSC Adv.,* 5 (2015) 91302-91307.
8. L. Z. Hu, Y. L. Yuan, L. Zhang, J. M. Zhao, S. Majeed, G. B. Xu, *Anal. Chim. Acta,* 762 (2013) 83-86.
9. Y. C. Zhang, Y. X. Liu, L. Su, Z. H. Zhang, D. Q. Huo, C. J. Hou, Y. Lei, *Sens. Actuators, B.,* 191 (2014) 86-93.
10. T. Dayakar, K. Venkateswara Rao, K. Bikshalu, V. Rajendar, S. H. Park, *Mater. Sci. Eng. C.,* 75 (2017) 1472-1479.
11. R. Prasad, N. Gorjizadeh, R. Rajarao, V. Sahajwalla, B. R. Bhat, *RSC Adv.,* 5 (2015) 44792-44799.
12. S. B. Hocevar, B. Ogorevc, K. Schachl, K. Kalcher, *Electroanalysis,* 16 (2004) 1711-1716.
13. M. B. Zheng, L. L. Li, P. Gu, Z. X. Lin, H. G. Xue, H. Pang, *Microchim. Acta,* 184 (2017) 943-949.
14. Y. C. Chen, J. H. Hsu, Z. B. Chen, Y. G. Lin, Y. K. Hsu, *J. Electroanal. Chem.,* 788 (2017) 144-149.
15. J. W. Xu, N. Xu, X. M. Zhang, P. Xu, B. Gao, X. Peng, S. Mooni, Y. Li, J. J. Fu, K. F. Huo, *Sens. Actuators, B.,* 244 (2017) 38-46.
16. Y. Fan, X. Yang, Z. Cao, S. F. Chen, B. Zhu, *J. Appl. Electrochem.,* 45 (2014) 131-138.
17. F. Y. Huang, Y. M. Zhong, J. Chen, S. X. Li, Y. C. Li, F. Wang, S. Q. Feng, *Anal. Methods,* 5 (2013) 3050.
18. X. Wang, C. Y. Ge, K. Chen, Y. X. Zhang, *Electrochim. Acta,* 259 (2018) 225-232.
19. X. F. Hu, J. Li, J. C. Wang, *ESC Electrochem. Lett.,* 3 (2014) D13-D15.
20. F. Jiang, S. Wang, J. J. Lin, H. L. Jin, L. J. Zhang, S. M. Huang, J. C. Wang, *Electrochem. Commun.,* 13 (2011) 363-365.
21. K. Li, G. L. Fan, L. Yang, F. Li, *Sens. Actuators, B.,* 199 (2014) 175-182.
22. S. K. Meher, G. R. Rao, *Nanoscale*, 5 (2013) 2089-2099.
23. P. Jiang, J. L. Chen, F. Borondics, P. A. Glans, M. W. West, C. L. Chang, M. Salmeron, J. H. Guo, *Electrochem. Commun.,* 12 (2010) 820-822.
24. E. M. Lombardia, L. Lapeire, V. Maurice, I. D. Graeve, K. Verbeken, L. H. Klein, L. A. I. Kestens, P. Marcus, H. Terryn, *Electrochem. Commun.,* 41 (2014) 1-4.
25. J. L. Kunze, V. Maurice, L. H. Klein, H. H. Strehblow, P. Marcus, *Corros. Sci.,* 46 (2004) 245-264.

26. J. B. He, X. L. Li, J. X. Lin, *Chin. J. Nonferrous Metals,* 7 (1997) 45-48.
27. J. M. Feng, Q. Y. Gao, L. Q. Xu, J. C. Wang, *Electrochem. Commun.,* 7 (2005) 1471-1476.
28. X. Y. Yan, Y. Gu, C. Li, B. Zheng, Y. R. Li, T. T. Zhang, Z. Q. Zhang, M. Yang, *Anal. Methods*, 10 (2018) 381-388.
29. S. Radhakrishnan, H. Y. Kim, B. S. Kim, *Sens. Actuators, B,* 233 (2016) 93-99.
30. A. Venkadesh, S. Radhakrishnan, J. Mathiyarasu, *Electrochim. Acta,* 246 (2017) 544-552.
31. M. M. Gao, H. Wang, S. Ji, Q. Zhao, B. G. Pollet, R. F. Wang, *Mater. Sci. Eng., C,* 95 (2019) 174-182.
32. J. W. Ma, J. Wang, M. Wang, G. L. Zhang, W. C. Peng, Y. Li, X. B. Fan, F. B. Zhang, *Nanomaterials,* 8 (2018) 73-81.
33. J. Wang, W. D. Zhang, *Electrochim. Acta,* 56 (2011) 7510-7516.
34. L. L. Li, Y. Y. Liu, L. H. Ai, J. Jiang, *J. Ind. Eng. Chem.,* 70 (2019) 330-337.
35. S. D. Sun, X. Z. Zhang, Y. X. Sun, S. C. Yang, X. P. Song, Z. M. Yang, *ACS Appl. Mater. Interfaces,* 5 (2013) 4429-4437.
36. W. Wang, L. L. Zhang, S. F. Tong, X. Li, W. B. Song, *Biosens. Bioelectron., 25* (2009) 708-714.
37. C. L. Li, Y. Su, S. W. Zhang, X. Y. Lv, H. L. Xia, Y. J. Wang, *Biosens. Bioelectron.,* 26 (2010) 903-907.
38. G. H. He, L. Wang, *Ionics,* 24 (2018) 3167-3175.
39. X. G. Ma, Q. Zhao, H. Wang, S. Ji, *Int. J. Electrochem. Sci.,* 12(2017) 8217-8226.
40. V. Vinoth, T. D. Shergilin, A. M. Asiri, J. J. Wu, S. Anandan, *Mater. Sci. Semicond. Process.,* 82 (2018) 31-38.